

ADVANTAGES OF HEXAGONAL SAMPLING GRIDS AND HEXAGONAL SHAPE DETECTOR ELEMENTS IN REMOTE SENSING IMAGERS

Bruno Aiazzi^a, Stefano Baronti^a, Annalisa Capanni^b, Leonardo Santurri^a, Raffaele Vitulli^c

^a "Nello Carrara" Research Institute on Electromagnetic Waves, CNR,
Via Panciatichi 64, I-50127 Firenze, Italy

^b Galileo Avionica, Via Einstein 35, 50013, Campi Bisenzio, Firenze, Italy

^c European Space Agency, Keplerlaan 1, 2200 AG, Noordwijk, The Netherlands

ABSTRACT

Recent improvements in CCD technology make hexagonal sampling attractive for such applications as remote sensing where the acquisition process is crucial to preserve image quality without introducing data transmission overheads. In the following hexagonal sampling is analyzed under general assumptions and compared with conventional rectangular sampling. The analysis takes into account both the lattice form (square, rectangular, hexagonal, regular hexagonal), and the shape of the single detector element. The hexagonal grid is not based a-priori on a regular hexagon tessellation, i.e., no constraint is made on the ratio between the sampling frequencies in the two spatial directions.

1. INTRODUCTION

The objective of this paper is to quantify the advantages of hexagonal sampling grid and hexagonal pixel shape with respect to conventional rectangular sampling and rectangular pixel shape. Sampling conditions are expressed for a generic hexagonal sampling grid, and a comparison is performed with sampling conditions for a corresponding rectangular lattice. Afterwards the comparison is performed under the assumption of same number of pixels for unity of surface, and the particular case of regular hexagonal sampling grid is considered. Regarding the single detector cell, the hexagonal and the rectangular shapes are examined. Finally, octagonal shape detectors are compared to rectangular and hexagonal ones.

2. HEXAGONAL LATTICE

Let us denote a generic hexagonal sampling lattice as that depicted in Figure 1 (left) as:

$$comb_{HEX} \left(\frac{x}{\Delta X'}, \frac{y}{\Delta Y'} \right) \quad (1)$$

Notice that the hexagonal sampling steps $\Delta X'$ and $\Delta Y'$ are defined as the distances between two consecutive columns

and rows, respectively. This definition is natural and useful for computational purpose, even if it is not handy to perform a comparison with a rectangular grid with sampling steps ΔX , ΔY . In fact, to have the same density of pixels on the two grids it should be $2(\Delta X' \Delta Y') = (\Delta X \Delta Y)$. No constraint is assumed for the ratio between $\Delta X'$ and $\Delta Y'$. The resulting sampling grid is based on a generic possibly irregular hexagonal geometry, the sampling points being the centers of the hexagons.

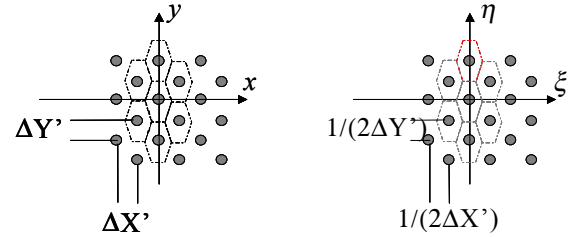


Figure 1: Hexagonal sampling grid and its Fourier Transform.

The Fourier Transform (FT) of a hexagonal lattice is still a hexagonal lattice [1] as that reported in Figure 1 (right).

$$\mathfrak{S} \left\{ comb_{HEX} \left(\frac{x}{\Delta X'}, \frac{y}{\Delta Y'} \right) \right\} = comb_{HEX} \left(\frac{\xi}{\left(\frac{1}{2\Delta X'} \right)}, \frac{\eta}{\left(\frac{1}{2\Delta Y'} \right)} \right) \quad (2)$$

In the FT domain, unlike rectangular lattices, in hexagonal lattices the inverse of the sampling steps correspond with the distances between two “aligned” rows and columns, that are twice the corresponding steps. The FT $G_{S-hex}(\xi, \eta)$ of the hexagonally sampled image is composed by infinite replicas of the spectrum of $G(\xi, \eta)$, FT of the image $g(x, y)$ to be sampled. These replicas are centered in the points of the hexagonal lattice (2) that is the FT of the hexagonal sampling lattice.

$$G_{S-hex}(\xi, \eta) = \sum_k \sum_l \left[G \left(\xi - \frac{k}{2\Delta X'}, \eta - \frac{l}{2\Delta Y'} \right) \right]$$

$$k + l = 2p \quad p \in N$$

If we assume that $g(x,y)$ is characterized by a band-limited spectrum with an elliptic support, a comparison between the spectrum of the sampled image in the two hypotheses of rectangular and hexagonal sampling can be performed as shown in Figure 2 in the case of equal pixel density.

If N_{rect} and N_{hex} are the pixel densities, i.e. the number of pixel for unity of surface for the detector array in the rectangular and hexagonal grids, respectively, it is easy to notice that $N_{rect}=1/(\Delta X \Delta Y)$ and $N_{hex}=1/(2\Delta X' \Delta Y')$. The same pixel density is so obtained when $\Delta X \Delta Y=2\Delta X' \Delta Y'$. If this constraint on the density in the spatial domain is verified, also the density of the replicas results the same.

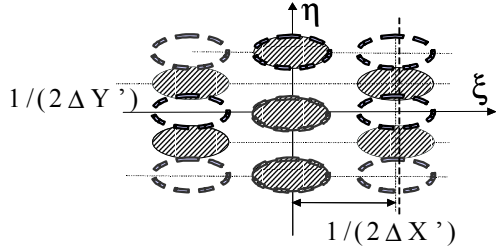


Figure 2: Projection onto the spatial frequencies plane of the FT of a hexagonally sampled image (filled) and of a corresponding rectangular sampling with same pixel density (dashed contour).

3. HEXAGONAL VS. RECTANGULAR LATTICE

Let us fix the values of ξ_{MAX} and η_{MAX} , for which $G(\xi,\eta)$ becomes null and find the sampling limits to avoid aliasing [2-3]. A comparison between these two Nyquist constraints in the rectangular and hexagonal case can be then performed by considering the limit values for the pixel densities: the less is the minimum density requested, the better is the sampling performance.

The minimum densities correspond to a packaging of the spectra as those reported in Figure 3 for the rectangular sampling and in Figure 4 for the hexagonal grid.

Thus, the hexagonal sampling avoids aliasing with a pixel density that is $\sqrt{3}/2$ and thus lower than rectangular one:

$$N_{rect-min} = 4\xi_{MAX}\eta_{MAX}$$

$$N_{hex-min} = 2\sqrt{3}\xi_{MAX}\eta_{MAX} = \frac{\sqrt{3}}{2} N_{rect-min} \quad (3)$$

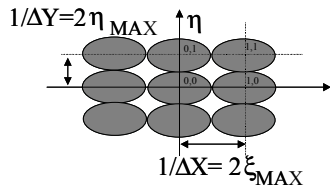


Figure 3: Spectral packaging for best rectangular sampling.

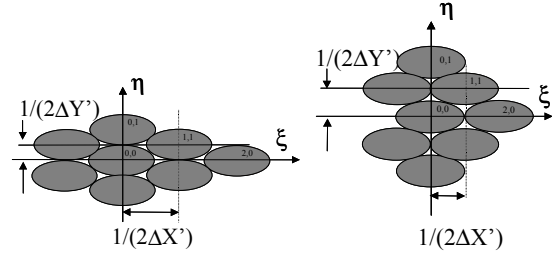


Figure 4: Spectral packaging for best hexagonal sampling.

4. SPECTRAL PACKAGING

Figure 4 shows the two hexagonal samplings that originate the closest and thus the best packaging of the replicas in the frequency domain. Nyquist conditions can be found in the general case of a hexagonal lattice originating a non optimal tangential packaging. Let us now consider the case of a signal whose spectrum possesses a circular support of radius R ($\xi_{MAX}=\eta_{MAX}=R$).

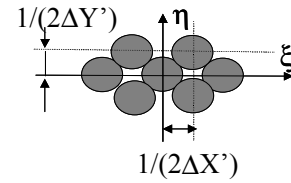


Figure 5: Tangential packaging for circular support spectrum.

The Nyquist conditions can be found by considering the generic tangential packaging of Figure 5 and result to be the following:

$$\begin{cases} \frac{1}{\Delta X'} \geq 2R & \text{i)} \\ \frac{1}{\Delta Y'} \geq 2R & \text{ii)} \\ \left(\frac{1}{2\Delta X'}\right)^2 + \left(\frac{1}{2\Delta Y'}\right)^2 \geq 4R^2 & \text{iii)} \end{cases}$$

Figure 6 graphically describes the constraints i) ii) and iii). The aliasing zone is filled. Since the geometric locus of constant pixel densities corresponds with a equilateral hyperbola, it is possible to demonstrate that i) ii) and iii) are always less stringent, i.e. related to a lower pixel density, than those of the rectangular sampling. Only for the point C of Figure 6 ($\Delta X'=\Delta Y'$) the pixel densities result the same for the two lattices at the Nyquist limit; in fact in this case the hexagonal lattice becomes a square lattice rotated by 45° . Under the assumption of circular support, the two optimal packaging of Figure 4 correspond to regular hexagonal lattices, and are represented by points A and B of Figure 6.

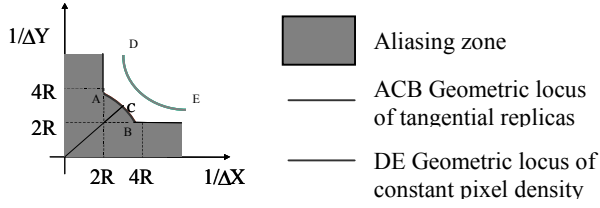


Figure 6: Nyquist conditions for hexagonal lattice.

5. REGULAR HEXAGONAL SAMPLING LATTICE

The adoption of a regular hexagonal grid results in a simple constraint between the sampling steps and the side L of the generic hexagonal cell of the grid.

$$\begin{cases} \Delta X' = \frac{3}{2}L \\ \Delta Y' = \frac{\sqrt{3}}{2}L = \frac{1}{\sqrt{3}}\Delta X' \end{cases}$$

Let us assume a circular spectrum for the image being sampled. The regular hexagonal lattice originates just the best packaging of the replicas as in Figure 4. The best case for the rectangular sampling lattice occurs when the lattice becomes square [4] as shown in Figure 7, where the same pixel density is assumed for both lattices.

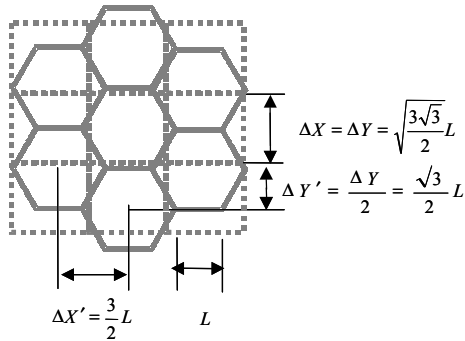


Figure 7: Square vs. hexagonal lattice.

In this case, if R_{HEX} and R_{SQR} denote the radius of the circular spectrum for the hexagonal and square lattice at the limit conditions of tangential packaging, it can be found that $R_{HEX} = 1.074 R_{SQR}$.

Thus, a wider spectrum signal can be acquired without aliasing by a hexagonal lattice. Conversely, the same signal can be acquired without aliasing by a hexagonal lattice with a lower pixel density. In particular it can be proven that (3) still holds, being $1/(1.074)^2$ the approximation of $\sqrt{3}/2$.

6. PIXEL SHAPE

Pixel shape also has an impact on the spectrum of the sampled image [5-6]. If the signal is assumed as band-

limited, the MTF (Modulation Transfer Function) should be ideal, i.e. equal to one inside the base-band. In the practice, detectors with rectangular shape elements with nearly uniform sensitivity are employed due to technological reasons. Recent developments in sensor technology make other pixel shapes attractive because of their MTF. The optimum pixel shape has to fulfill some requirements: trivially the MTF should be not only ideal but also symmetric. The symmetry of the shape is a strong requirement, since an asymmetric shape is related to an asymmetric pre-filtering behavior. The SNR is another parameter that can be considered. Since high values of the SNR are desirable, a pixel shape that permits a high fill factor is preferable. In the following, the MTF of a hexagonal (regular) pixel shape is analyzed and compared with the MTF of a corresponding rectangular shape.

7. HEXAGONAL VS. RECTANGULAR SHAPE

To analyze the MTF of both rectangular and hexagonal shapes, let us consider the sampling grid of Figure 8 in which a regular hexagonal lattice of side L is analyzed, with a rectangular and a hexagonal pixels shape. The two shapes have the same centers and the same areas.

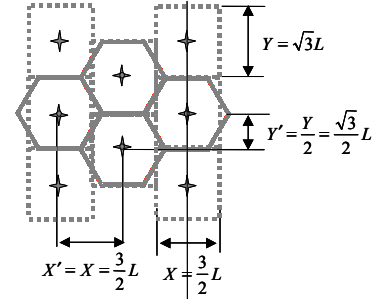


Figure 8: Rectangular vs. hexagonal shape.

The MTF of a rectangular shape detector cell is separable:

$$\begin{cases} MTF'_{RECT}(\xi, 0) = MTF'^y_{RECT}(\xi) \approx \text{sinc}\left(\frac{3L}{2}\xi\right) \\ MTF'_{RECT}(0, \eta) = MTF'^x_{RECT}(\eta) \approx \text{sinc}(\sqrt{3}L\eta) \end{cases} \quad (4)$$

The MTF of a hexagonal pixel shape is not separable and cannot be decomposed in sections along axes. Anyway, a comparison can be performed by examining these two sections with the corresponding sections of the MTF referred to the rectangular shape:

$$\begin{cases} MTF'_{HEX}(\xi, 0) = MTF'^y_{HEX}(\xi) = \left[\text{sinc}\left(\frac{L}{2}\xi\right) \cdot \text{sinc}\left(\frac{3L}{2}\xi\right) \right] \\ MTF'_{HEX}(0, \eta) = MTF'^x_{HEX}(\eta) = \frac{2}{3} \left[\frac{1}{2} \text{sinc}^2\left(\frac{\sqrt{3}L}{2}\eta\right) + \text{sinc}(\sqrt{3}L\eta) \right] \end{cases} \quad (5)$$

By comparing 4 and 5 in the limit condition for aliasing appearance in the case of a regular hexagonal lattice (i.e. $\xi = \eta = 1/(2\Delta X') = 1/(3L)$), we have [7]:

$$\left\{ \begin{array}{l} MTF'^y_{RECT} \left(\frac{1}{3L} \right) = 0.636 \\ MTF'^x_{RECT} \left(\frac{1}{3L} \right) = 0.535 \end{array} \right. \quad \left\{ \begin{array}{l} MTF'^y_{HEX} \left(\frac{1}{3L} \right) = 0.608 \\ MTF'^x_{HEX} \left(\frac{1}{3L} \right) = 0.608 \end{array} \right.$$

The MTF resulting from a hexagonal pixel shape along the x direction is about 4.8% lower than the MTF of a rectangular pixel shape while the MTF along the y direction is about 13.6% higher. In addition the hexagonal pixel shape MTF is approximately equivalent in both x and y directions. Since the MTF has to be as equal to one as possible, the hexagonal pixel shape results better along the y direction and worse along the x direction; a 2-D analysis can show that the hexagonal pixel shape MTF exceeds the MTF of the rectangular pixel shape over most of the base-band. In any case it is fair to notice that the MTF of a detector element is a good and common way to analyze the effects of the pixel shape, but not completely satisfying to measure the effect of over-sampling and to describe the pixel shape impact onto the quality of the oversampled signals, as it only allows for pixel shape and size, and not for the relative position between pixels. Concerning symmetry, it is trivial to notice that a regular hexagonal pixel shape is more symmetric (of a 50%) than a square pixel, since it exhibits 12-fold as opposed to 8-fold symmetry. Further, the hexagonal sampling has three axes of symmetry (0° , 60° and 120°) in the frequencies domain, as opposed to the two in the rectangular grid; this symmetry results useful for computational tasks (25-50% more efficient), such as filter design.

8. OCTAGONAL VS. RECTANGULAR SHAPE

Octagonal shape has been adopted in recent CCD sensors. The best mapping is reached by means of a square sampling lattice with a fill factor of 82%; the number of symmetry axes increase to 16. Analogously to the hexagonal shape detector element it is possible to compare the octagonal shape with side L_{OCT} , with a rectangular shape on a square lattice.

By considering the MTF' in the limit condition for aliasing appearance for the square and the octagonal shape, both referred to the same square lattice with sampling step of $L_{OCT}(1+2^{1/2})$, i.e. on the base-band border, we have [4]:

$MTF'^y_{SQR} \left(\frac{1}{2L_{OCT}(1+\sqrt{2})} \right) = 0.636$	$MTF'^y_{OCT} \left(\frac{1}{2L_{OCT}(1+\sqrt{2})} \right) = 0.684$
$MTF'^x_{SQR} \left(\frac{1}{2L_{OCT}(1+\sqrt{2})} \right) = 0.636$	$MTF'^x_{OCT} \left(\frac{1}{2L_{OCT}(1+\sqrt{2})} \right) = 0.684$
$MTF'^d_{SQR} \left(\frac{1}{2L_{OCT}(1+\sqrt{2})} \right) = 0.655$	$MTF'^d_{OCT} \left(\frac{1}{2L_{OCT}(1+\sqrt{2})} \right) = 0.684$

Where MTF'^d refers to the diagonal (45°) direction.

This results in a better performance of the octagonal shape detector along axes and diagonal directions. So, octagonal shape shows a better performance from the symmetry and the MTF point of view with respect to the square shape.

9. CONCLUSIONS

Hexagonal sampling lattice offers better performance than the rectangular one. Wider spectra can be sampled without aliasing with the same pixel density, or less number of pixels are needed to sample the same signal. This allows a wider area for each detector element, with an improvement in the SNR and in the low-pass pre-filtering capabilities. Hexagonal sampling lattices permit to use a hexagonal sampling shape with a theoretical fill-factor of 100%, and this kind of shape results better from MTF and from symmetry considerations. Hexagonal pixel shape better approximates a circular band-region than a rectangular. The regular hexagon symmetry may result useful for computational tasks, such as filtering. Hexagonal pixel shape involves three axes of symmetry (0° , 60° , and 120°) in the spatial frequencies domain, as opposed to the two of the rectangular one. Octagonal shape has a fill factor that is not 100%, and is related to a square lattice, but it is more symmetric and performs better than a square shape.

10. ACKNOWLEDGMENT

This work was realized under the ESA contract “*Study on Coupling Radiometry-Image Quality for Hyperspectral Applications*”, undertaken by Galileo Avionica and IROE-CNR. A particular thanks to A. Barducci, I. Pippi from IROE-CNR and U.Del Bello from ESA.

11. REFERENCES

- [1] W. Goodman, Introduction to Fourier Optics, McGraw Hill, 1996.
- [2] H. Nyquist, “Certain topics on telegraph transmission theory”, Tr. of American Institute of Electrical Engineers, vol. 47, pp. 617-644, 1928.
- [3] C.E. Shannon, “Communication in Presence of Noise”, Proc. of the I.R.E., vol. 37, pp.10-21, January 1949.
- [4] S. Baronti, A. Capanni, A. Romoli, L. Santurri, R. Vitulli, “On detector shape in hexagonal sampling grids”, in “Sensor, Systems, and Next Generation Satellites VII”, SPIE 8th Int. Symp. on Remote Sensing, Toulouse, France, 2001, in press.
- [5] G. Holst, “Sampling, aliasing, and data fidelity”, SPIE Press, Bellingham, 1998.
- [6] K. Barnard, G. Boreman, “Modulation transfer function of hexagonal staring focal plane arrays”, Opt. Eng., 30(12), pp. 1915-1919, December 1991.
- [7] O. Hadar, G. Boreman, “Oversampling requirements for pixelated-imager systems” Opt. Eng., 38(5), pp. 782-785, May 1999.